Journal of the Korean Society of Remote Sensing, Vol.15, No.4, 1999, pp.321~327

Detecting red tides in turbid waters

Sin-Jae Yoo* and Jong-Chul Jeong**

Korea Ocean Research Development Inst.*, NamSeoul University Dep. of Geoinformatic Engineering**

Abstract : As an example of many possible applications of OSMI data, we present a method to detect red tides. In Korean waters, red tides usually occur in the South Sea where the turbidity is usually high due to strong tidal mixing in the shallow sea. The conventional case 1 chlorophyll algorithm cannot be applied since it cannot distinguish chlorophyll from SS (suspended sediments). In October 1998, a red tide outbreak occurred off the coast of KunSan. We analyzed the SeaWiFS data of the outbreak. The standard SeaWiFS chlorophyll algorithm OC-2 was poor in identifying the red tides. However, comparison of spectra of normalized water-leaving radiance indicates that red tide pixels can be distinguished from sediment-laden pixels. Channel 443 and 555 were effective in showing the spectral characteristics. We suggest K490 algorithm as an example in summarizing the information of the spectra and thereby in distinguishing the red tide pixels. Further development is desirable.

Key Words : red tides, coastal area, turbid water

1. Introduction

We have studied potential application of OSMI ocean color sensor on KOMPSAT in Korean coastal waters. SeaWiFS and OCTS data, which have comparable characteristics with OSMI have been analyzed. The areas of interest were monitoring and mapping of 1) primary productivity, 2) red tides, 3) Changjiang outflow, and 4) SS (suspended sediment) in Korean waters. Among them here we present a method of identifying red tide pixels in Korean waters.

The simplest way of detecting red tides is to take advantage of high chlorophyll concentration. This, however, does not work in Korean waters since most red tides plagued region in Korean waters belong to case 2 waters. In the South Sea and the Yellow Sea it is shallow and tidal mixing is very strong and as a result SS concentration is also high. The standard SeaWiFS chlorophyll algorithm uses the ratio of the water-leaving radiance of the band 3 (490nm) and the band 5 (550nm). Chlorophyll decreases the band 3 out of proportion reducing this ratio. The problem using this algorithm is that SS will also reduce the ratio by increasing the band 5. We present a method that can distinguish red tides pixels in the presence of high SS loads.

2. Materials and methods

In October 1998, a red tide outbreak occurred and continued for a month in the region off the

Received 6 October 1999 ; Accepted 15 November 1999.

coast of Kun-San. SeaWiFS level 0 data of October 23, 1998 received at KORDI station was processed by SeaDAS 3.2. The following algorithms were used(Fig. 1).

$$Chl = -0.04+10^{(0.341-3.001x+2.811x^2-2.041x^3)} \quad (1)$$

$$K_{490} = 0.022(0.1\frac{L_2}{L_5})^{-1.2996} \quad (2)$$

where $x = \log_{10}[R_{rs}(490) / R_{rs}(555)]$,

$R_{rs}(\lambda)$: remote sensing reflectance

Chl: Chlorophyll-a concentration (mg m^{-3})

L_{wn}: Atmospherically-corrected normalized water-leaving radiance (mW sr^{-1} cm^{-2} μm^{-1}),

$L2 = 443$, $L5 = 555$ (nm)

3. Results

The red tides patches were observed near Kun-San coast and Wi-Do island. Approximate

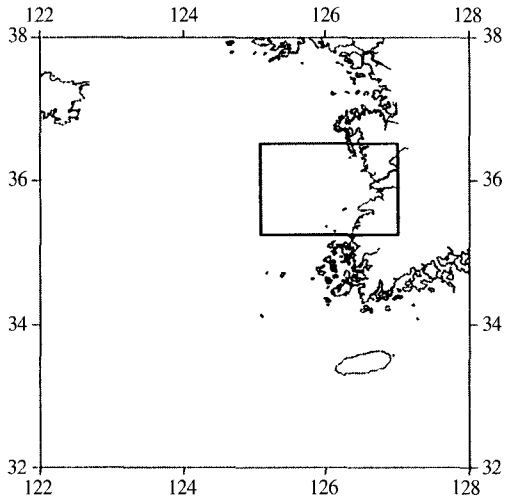

Fig. 1. Study area is indicated by a rectangle.

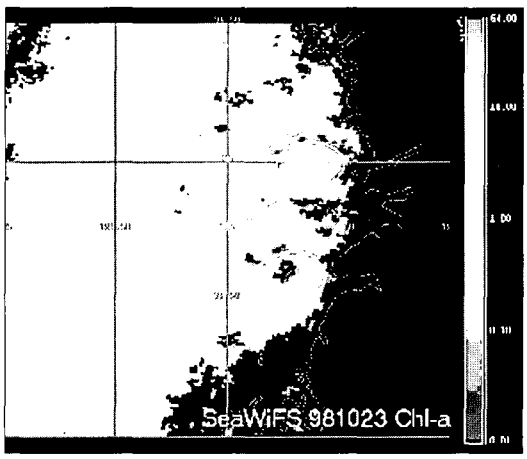

Fig. 2. Chlorophyll image by OC-2 algorithm.

location of these patches is corresponded with very high chlorophyll concentration (indicated by circles; > 10 mg m^{-3}) in Fig. 2. Fig. 2 shows the chlorophyll concentration calculated using OC-2 algorithm (1). Along the coastal line, the chlorophyll concentration appears high (>~5.0 mg m^{-3}). It is evident, however, that not all these pixels are of high chlorophyll concentration and most pixels represent overestimated values due to high SS concentration.

Inspecting each band, however, reveals interesting features. Channel 443 is low in the open waters but high along the whole coastal line due to high SS concentration (Fig. 3). Within this high reflectance strip, there are two patches of low radiance (represented by arrows) suggesting that blue-light absorbing is strong, which in turn indicates the presence of high density of red tide organisms.

The channel 555 shows similar pattern with the channel 443 (Fig. 4). Very high L_{wn} indicates high SS loads. There are, however, discrepancies in a few locations where channel 555 is very high but channel 443 is low (indicated by arrows). Thus

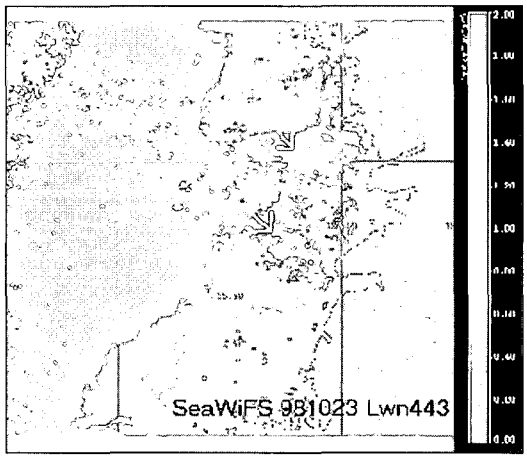

Fig. 3. Channel 443 nm image.

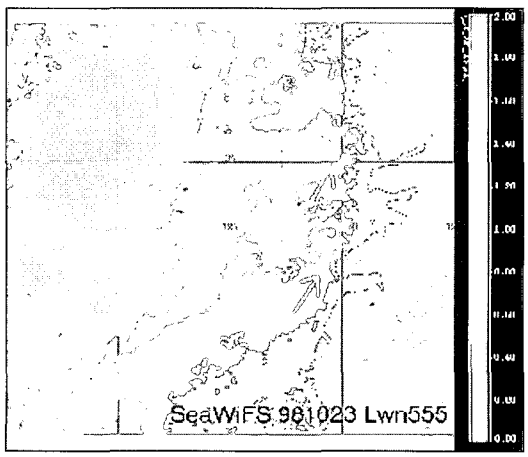

Fig. 4. Channel 555 nm image.

there appear two types of red tides pixels; with moderate level of reflectance in 555nm and very high level of SS concentration.

Based on this, the whole scene can be divided into four types; 1) open waters with less SS and chlorophyll, 2) the water with high SS, 3) red tide water with moderate level of SS, and 4) red tide water with high level of SS.

From representing pixels of the four types, spectra of L_{wn} were reconstructed. Open waters show spectra typically observed in the Yellow Sea (Fig. 5, Yoo and Park, 1998). The peak is at 490 nm and it decreases at longer wavelengths. Open water with high SS concentration shows spectra where L_{wn} at 510 and 555nm are raised to the same level as the 490nm (Fig. 6). The magnitude of the whole spectra is also greatly increased.

The water with red tides shows spectra where the L_{wn} increases towards longer wavelengths (Fig. 7). When the red tide water is mixed with high SS, the shape of the spectra remains the same

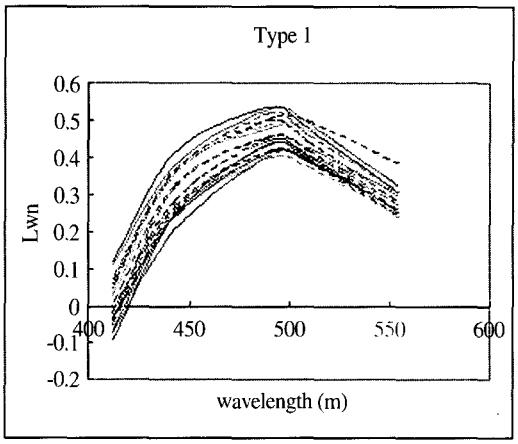

Fig. 5. L_{wn} Spectra of open water pixels.

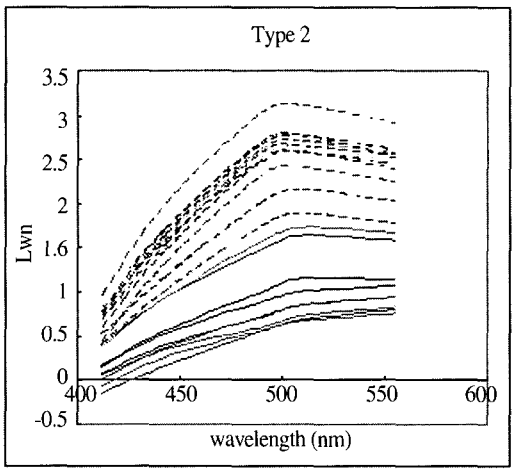

Fig. 6. L_{wn} spectra of water with high SS.

while the overall magnitude increases (Fig. 8). This is consistent with previous study (Yoo and Park, 1998), where chlorophyll concentration and SS concentration were high. This is also comparable with the results obtained in turbid lakes (Bukata *et al.*, 1981a, 1981b).

Therefore the shapes of the L_{wn} spectra of the four water types fall into three basic types. The shapes are different largely in green band (510 and 555nm). With the open water type, the green band is decreasing. With high SS water, green band is flat. With red tide water, the green band is increasing regardless of SS concentration.

It follows that 443nm and 550nm would be the best channels that distinguish the three spectra shapes. Fig. 9 is a scattered plot of the four type pixels on 443 vs 555nm plane. On this plot, the four types of pixels are distinctively segregated. Scatter of high SS water is very small (R^2 = 0.99). Red tide pixels regardless of SS level aggregate with the same slope (R^2 = 0.84).

We calculated K_{490} (2) whose algorithm utilizes 443 and 555nm. In the K_{490} image, red tide patches. are well identified. Red tide patches are

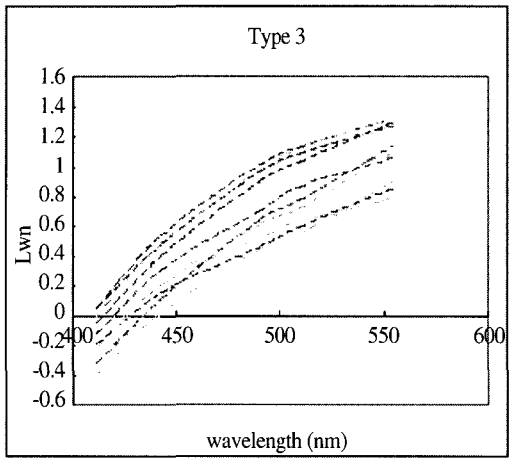

Fig. 7. L_{wn} spectra of red tide water.

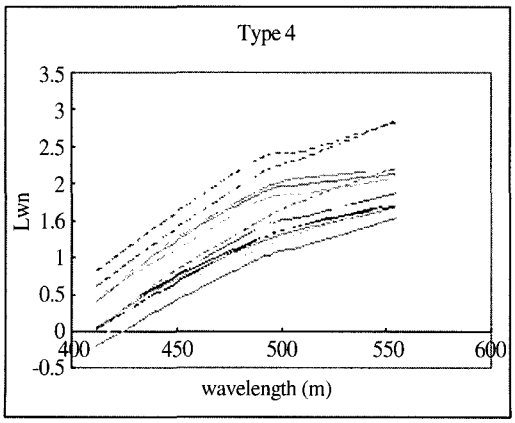

Fig. 8. L_{wn} spectra of red tide pixels with high level with SS.

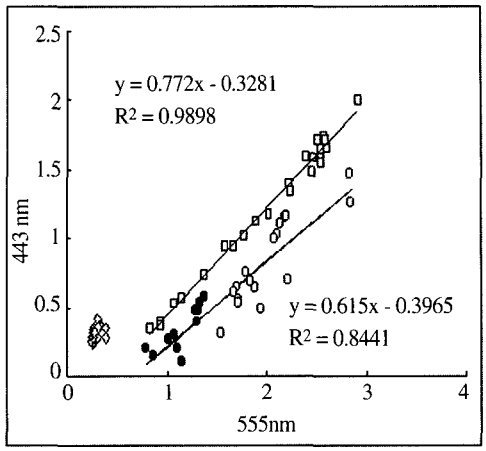

Fig. 9. Scattered plot of the four spectra types on 443-555 nm plane. Diamonds : open water, rectangles : high SS water, filled circles : red tide water with less SS, and open circles : red tide water with high SS.

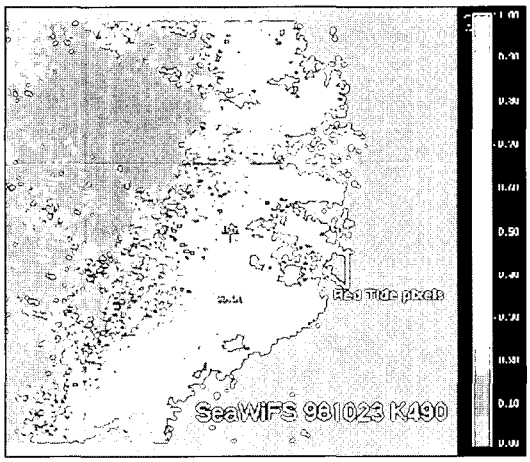

Fig. 10. K_{490} image.

clearly distinguished from adjacent pixels by very high value (> ~1.0 m^{-1}). K_{490} algorithm is for case 1 waters, therefore it does not give correct values in case 2 waters. However, SS pixels assume low K_{490} values while red tide pixels show high K_{490} values. This can be utilized in distinguishing red tide pixels from SS in case 2 waters (Fig. 10.).

4. Conclusions

Ocean color in coastal waters presents complicated problems: atmospheric correction, and in-water algorithm. During the absence of ocean color sensors, some researchers tried to use AVHRR to detect red tide patches (Stumpf and Tyler, 1988; Gower, 1994). They used band 2 to correct for atmospheric noise by subtracting band 2 from band 1. As seen in Fig. 8, when chlorophyll increases, reflectance at longer wavelength, e.g. > 500nm, also increases. So red tides patches might appear as "bright pixels" (Gower, 1994). These attempts were successful only to the extent that AVHRR's sensitivity allows. This method was

also severely limited in turbid waters since when SS was high, atmospheric correction was overdone.

One might expect ocean color sensors with more channels and higher sensitivity would prove to provide better information. As in this study, spectra of L_{wn} can be retrieved. However, quantitative analysis requires correct atmospheric correction. The currently used atmospheric correction scheme of ocean color remote sensing, e.g., SeaWiFS algorithm (Gordon and Wang, 1994) is based on the assumption that water-leaving radiance in NIR region (700~900nm) is effectively zero. This assumption is unwarranted in turbid waters and when applied, could result in an underestimation of water-leaving radiance. This is evident in the L_{wn} spectra presented here (Fig. 6-8).

In the absence of appropriate atmospheric correction and in-water algorithm in turbid waters, such method presented here would be a practical approach. K_{490} is has limitations and further development is desirable in this direction.

References

Bukata, R. P., J. H. Jerome, J. E. Bruton, and H. H. Zwick, 1981a, Optical water quality model of Lake Ontario. 1: Determination of the optical cross sections of organic and inorganic particulates in Lake Ontario, *Applied Optics*, 20(9):1696-1703.

Bukata, R. P., J. H. Jerome, J. E. Bruton, and H. H. Zwick, 1981b, Optical water quality model of Lake Ontario. 2: Determination of chlorophyll a and suspended mineral concentrations of natural waters from submersible and low altitude optical sensors, *Applied Optics*, 20(9):1704-1714.

Gordon, H. R., M. Wang, 1994, Retrieval of water-leaving radiance and aerosol optical thickness over the oceans with SeaWiFS: a preliminary algorithm, *Applied Optics*, 33(3):443-452.

Gower, J. F., 1994, Red tide monitoring using AVHRR HRPT imagery from a Local Receiver, *Remote sensing of Environment* 48:309-318.

Stumpf, R. P., M. A. Tyler, 1988, Satellite detection of bloom and pigment distributions in Estuaries, *Remote Sensing of Environment*, 24: 385-404.

Yoo, S. J. and J. S. Park., 1998, Bio-optical properties in the Yellow Sea, *J. of Korean Society of Remote Sensing*, 14(3):285-294.